JOURNAL OF MATERIALS SCIENCE **38** (2003) 2979–2986

Coagulation/phase separation process in the silica/inorganic salt systems (1)—observation of state transformation—

K. IMAIZUMI*
Department of Materials Science and Engineering, Shibaura Institute of Technology, Shibaura 3-9-14, Minato-ku, Tokyo 1088548, Japan; Corporate Research and Development Administration, Asahi Chemical Industry Co., Ltd., 1-1-2 Yuraku-cho, Chiyoda-ku, Tokyo 100-8440, Japan
E-mail: m699502@sic.shibaura-it.ac.jp

N. MATSUDA, M. OTSUKA
Department of Materials Science and Engineering, Shibaura Institute of Technology, Shibaura 3-9-14, Minato-ku, Tokyo 1088548, Japan

The authors investigated the transformation of state of silica particles and inorganic salts during the calcination of solid mixtures of silica/potassium halide (KX), which separated the mixture components producing microporous structures, at temperatures below the melting point of either materials. The silica sol (SiO_2–Na_2O)/KX solid was examined at high temperatures using thermal analysis, X-ray diffractometry (XRD) and scanning electron microscopy (SEM). The data suggest the crystalline inorganic salt component transformed into an amorphous state ca. 100–200°C lower than its melting point, while the silica particle component coagulated, spontaneously separating the two components ("coagulation/phase separation"). Upon cooling, the inorganic salt was dispersed in water, resulting in porous silica with a narrow pore size distribution. However, at calcination temperatures above 800°C, formation of silica crystal existed as a separate domain without creating porous structures.

1. Introduction

Technologies for controlling form and structure have attracted much interest in the materials industry, as precise morphological control of various organic and inorganic materials is possible using present material manufacturing processes such as catalytic synthesis, asymmetric reactions, living polymerization, and organic/inorganic hybrid reactions. In particular, porous materials have been featured as an example of morphology control at the microscopic level.

There were no reports of materials having a porous structure at or below the microscopic level until zeolite was discovered by the Swedish scientist Cronstedt in 1756. Since then, many kinds of natural or synthetic zeolite possessing various pore sizes have been reported. However, all the zeolite pore sizes have been smaller than 1.5 nm.

Recently, many new porous materials with pores sizes in the mesoscopic and microscopic range have been reported, including materials synthesized with molecular self-assembly using mixtures of organic and inorganic materials [1–11]. Typical examples employing molecular self-assembly are three-dimensional biphase arrays synthesized with a variety of surfactants and inorganic phase precursors, which have been independently developed by Mobil and Waseda University/Toyota Central Laboratory [12–14]. Mobil's mesoporous materials (M41S) include hexagonal cylindrical structures having "mesoporous tubes" with $p6m$ space groups (MCM-41), cubic structures with $Ia\bar{3}d$ space groups (MCM-48), and lamella structures with L_α spaces (MCM-51) [15, 16].

We have already tried to control external particle size, and have successfully developed technology to control particle size on a micrometer level [17, 18]. In terms of internal shape control, porous materials have been obtained from a mixture of silica sol composed of particle sizes of 10 to 20 nm, with several kinds of water-soluble inorganic salts, through a spinodal decomposition-like process [19–22]. In this study, we found that the porous structures were initially formed by coagulation of the silica sol, which simultaneously resulted in phase separation of the silica and inorganic salt, at temperatures lower than the melting point of either mixture material. This "coagulation/phase separation" process clearly differed from the conventional process of pore formation that occurs above the melting point of silica in that coagulation occurred while the

*Author to whom all correspondence should be addressed.

silica and inorganic salt remained in a heterogeneous state without first entering into a homogeneous state. In this report, we focus on elucidating the state of transformation through this coagulation/phase separation process using solid mixtures of silica and inorganic salts.

2. Experimental

2.1. Preparation of starting materials

A commercially available silica sol (liquid) was used, possessing a spherical shape with an average diameter ranging from 10 to 20 nm (Snowtex^{TM} ST-30 colloidal silica: 30 wt% of SiO_2 and 0.6 wt% of Na_2O, Nissan Chemical Industries, Japan). Several kinds of inorganic salts were used as pore-size controllers. The pH of the silica sol solution was adjusted from a range of 9.5 to 10.5 to a pH of 4.0 to 5.0 by adding nitric acid. Then, an inorganic salt (solid) was added to the solution while stirring with an electromagnetic induction stirrer. The weight ratios of the starting materials for the silica/inorganic salt systems examined are summarized in Table I.

2.2. Syntheses of porous materials

As illustrated in Fig. 1, ca. 80 cm^3 of SiO_2/inorganic salt mixture solution was placed in a Petri dish, and dried at 80°C. A lump of mixture solid was crushed and screened with sieves from 70 to 300 mesh. The granular samples were calcined at a temperature between 500°C to 800°C for several hours using a tubular furnace (EKRO-23K, Isuzu Seisakusho, Japan). After cooling overnight to room temperature, the samples were placed into hot water (ca. 80°C), and then stirred with a magnetic stirrer for 10 min to leach the inorganic salt component from the samples.

2.3. Measurement of pore size and pore size distribution

Pore size (diameter) and pore size distribution were measured using a mercury-injected porosity meter (Pore Sizer 9320, Micromeritics, Japan). A sample (0.2–0.4 g) was placed into a sample cell, which was then placed into the lower-pressure chamber. The chamber was evacuated, and mercury was continuously poured into the chamber as the inner pressure of the chamber was returned to atmospheric pressure. The sample cell was then transferred to the high-pressure chamber, and the inner pressure was increased to 207 MPa.

TABLE I Composition of the starting materials[a]

SiO_2-Na_2O/KX	SiO_2/wt%	KX/wt%	Melting point of KX/°C
SiO_2-Na_2O/KCl	27.0	73.0	776
SiO_2-Na_2O/KBr	24.8	75.2	730
SiO_2-Na_2O/KI	23.1	76.9	723

[a]The mixture of silica (SiO_2)/KX was prepared with the volume fraction of SiO_2/KX = 30/70.

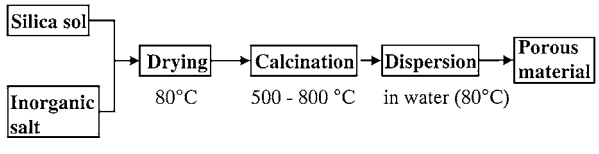

Figure 1 Schematic of porous material preparation.

2.4. Observation of the pore structure

The sample pore structures were observed using a scanning ion microscope (SIM) after cross-sectioning the samples with a focused ion beam (FIB) system (FIB-2000A, Hitachi Seisakusho, Japan). The FIB employed Ga ions at an acceleration voltage of 10–30 kV and a maximal current density of 15 A/cm^2. The resolution was set to less than 10 nm. To prevent the samples from charging up, the surfaces were coated with gold using an ion coater (IB-3, Eiko Engineering, Japan).

2.5. Determination of the crystalline state in the silica/KX mixture

The diffraction pattern of the silica/KX mixture was obtained using an X-ray diffractometer (XRD) (XRD-6100, Shimazu Seisakusho, Japan) equipped with a heat attachment (HA-1001) to raise the temperature during recording from room temperature to a temperature over the melting point (T_m) of inorganic salts. After drying the silica/inorganic salts completely, the powdery samples were placed on the stage of the heat attachment. The analysis conditions were as follows: X-ray source: Cu K_α (acceleration voltage: 40.0 kV; acceleration currency: 40.0 mA), slit divergence: 1°; scattering:1°; receiving: 1°, scanning diffraction angle (2θ) ranging from 0 to 60°; step: 0.02°; counting time: 0.5 s.

2.6. Differential thermal analysis (DTA)/thermogravimetry (TG)

To clarify the transition of state during the calcination process, a combination differential thermal analyzer/thermogravimeter (DTA-50, Shimazu Seisakusho, Japan) was employed for DTA/TG analysis of each silica/KX system. Ca. 10 mg of sample material was placed in the platinum cell, and heated at a temperature rate of 10°C/min from room temperature to 800°C under flowing N_2 (20 cm^3/min).

2.7. Observation of the coagulation/phase separation in the silica/inorganic salt system through the calcination process

To observe the state of the silica and inorganic salt phases during calcination, samples were heated while observations were conducted using an environmental scanning electron microscope (ESEM) (XL30ESEM-FEG, Nikon Instech, Japan). The sample was placed on the heating stage and heated at a temperature rate of 30°C/min from room temperature to 800°C. The ESEM observation conditions were as follows: accelerating voltage: 20 kV; emission current: 110 mA; pressure: 200 Pa; atmosphere: air.

3. Results and discussion

This study showed that a porous structure could be formed from a mixture of silica/inorganic salt under calcination temperatures lower than the melting temperature of either component. Cross-sections of the porous species were observed using SIM, XRD and ESEM. Based on these results, we suggest the transformational process as described below.

3.1. Pore diameter and pore size distribution of the calcined species from using various inorganic salt as pore size controllers

To prevent inter-particle siloxane bonding in silica sols, Na_2O is added as a stabilizer [23]. It is not clear whether the concentration of Na_2O affects the coagulation in the silica/inorganic salt (KX) system. However, in a separate experiment calcination of silica sol alone did not form porous structures under the same calcinations temperature condition used in the silica/inorganic salt systems. Thus, the effect of inorganic salt (KX) mixed with silica sol on the coagulation of the silica particles is considered to be different from that of Na_2O. To clarify the relationship between the formation of porous structure and the calcination temperature in the silica/KX systems, the pore size was determined for each species formed after calcination at various temperatures with different inorganic salts as pore size controllers.

Fig. 2a shows the pore diameter and pore size distribution in the case of silica/KCl ($T_m = 771°C$) calcined at temperatures of 600°C, 700°C, and 800°C for two hours. At 600°C, which was ca. 170°C lower than the melting point of the pore size controller (KCl in this case), a porous structure was formed with a narrow pore size distribution. In the case of a calcination temperature of 700°C, the mean pore diameter was ca. 43 nm and the pore size distribution was also found to be narrow. However, at a temperature of 800°C, few pores with a broad pore size distribution were observed.

Next, Fig. 2b shows the pore diameter and the pore size distribution for temperatures of 600°C, 700°C, and 800°C in the case of silica/KBr ($T_m = 734°C$) for two hrs. The mean pore diameters were 25 nm (at 600°C), and 60 nm (at 700°C) with a narrow pore size distribution. At 800°C, however, the pore size distribution was found to be broad, similar to the silica/KCl system.

Fig. 2c shows the pore diameter and the pore size distribution using silica/KI ($T_m = 723°C$) calcined at temperatures of 600°C, 700°C, and 800°C for two hours. At calcination temperatures of 600°C and 700°C, the mean pore diameters were ca. 25 nm and 60 nm, respectively. In the case of the silica/KI system, porous structures were not constructed at the calcination temperatures of 600°C, 700°C and 800°C (further described below).

3.2. Cross-sectional observation of the porous silica

To visually examine the shape of the porous structure in the calcined species, FIB cross-sectioned specimens were observed using SIM.

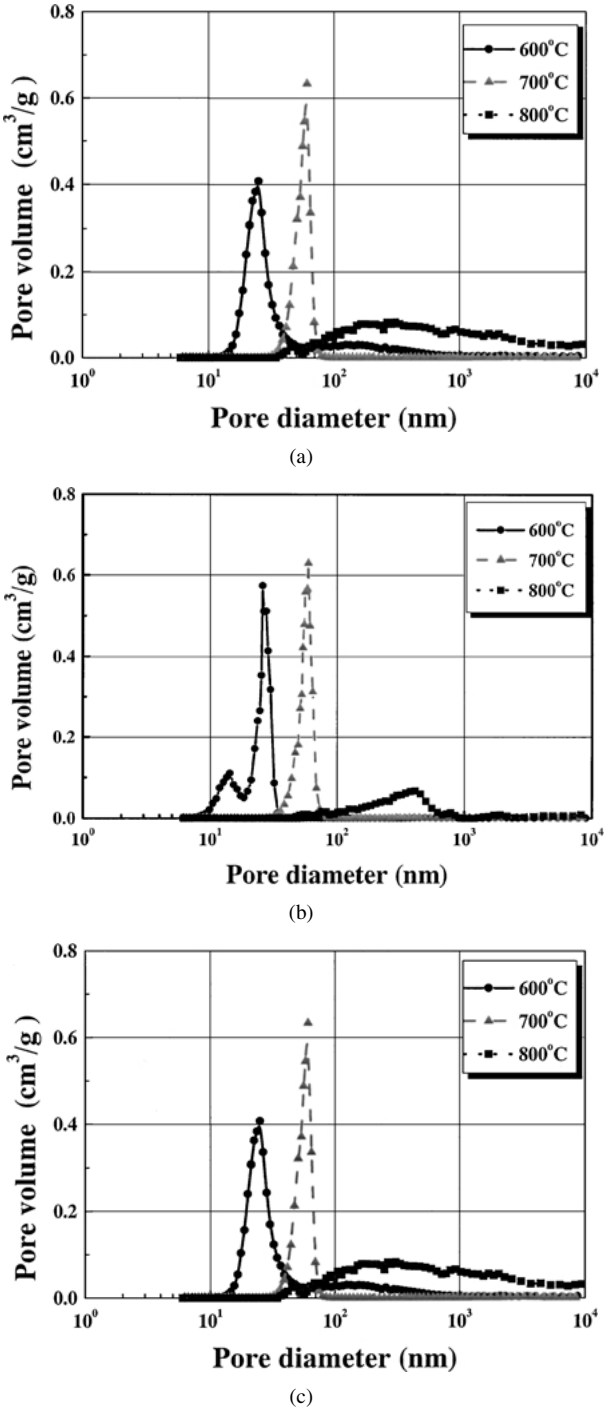

Figure 2 Pore size (diameter) and pore size distribution of porous silica formed from a silica/KX system: (a) silica/KCl, (b) silica/KBr, and (c) silica/KI.

Fig. 3a shows the SIM photographs of the cross sections of porous silica from the silica/KCl system formed at the calcination temperatures of (a) 600°C, (b) 700°C, and (c) 800°C. At 600°C, none of the pores could be observed because the pore diameters were too small to be individually identified. At 700°C, fine porous structures could be observed. At 800°C, however, macroscopic phase separation occurred between the silica phase and the inorganic salt phase.

Fig. 3b presents the SIM photographs of cross-section of porous silica from the silica/KBr system at temperatures of (a) 600°C, (b) 700°C, and (c) 800°C, respectively. Similar structures to those formed in the silica/KCl system were observed. Porous materials were

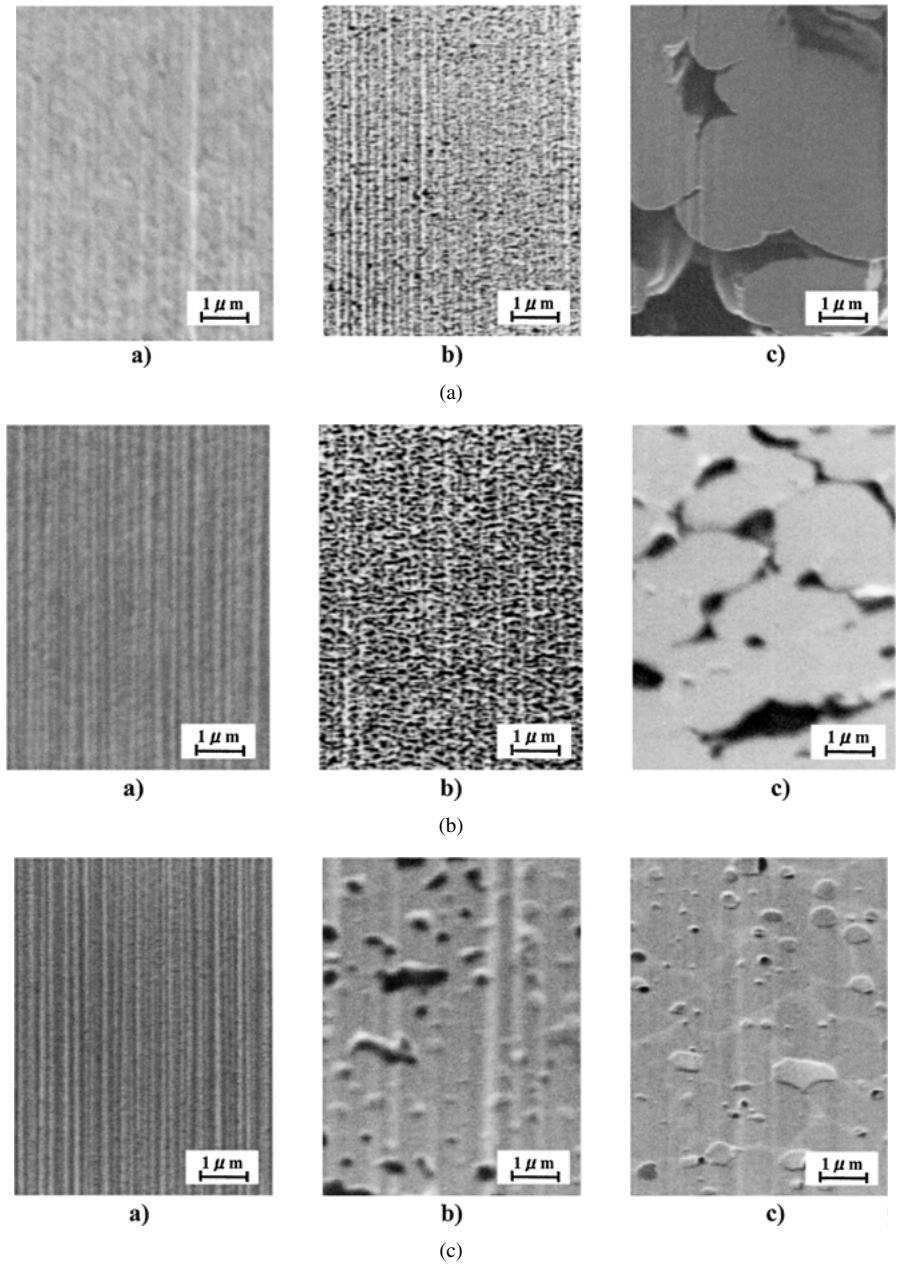

Figure 3 SIM photographs of cross-sections of porous silica formed from a silica/KX system. (a): silica/KCl calcined at (a) 600°C, (b) 700°C, and (c) 800°C. (b): silica/KBr calcined at (a) 600°C, (b) 700°C, and (c) 800°C. (c): silica/KI calcined at (a) 600°C, (b) 700°C, and (c) 800°C.

found to form at temperatures ranging from 100°C to 200°C below the melting point of the salts.

Fig. 3c shows the SIM photographs of the cross-sections of porous silica formed in the silica/KI system at the calcination temperatures of (a) 600°C, (b) 700°C, and (c) 800°C. In the silica/KI system, pores were not observed at any of the temperatures, but separated domains were clearly induced to form in the calcined species at each of these temperatures.

3.3. Thermal analyses

To clarify the transformation of state during the calcination process, DTA/TG analyses were also performed on the (a) silica/KCl, (b) silica/KBr, (c) silica/KI systems and (d) silica (blank) as shown in Fig. 4.

From the DTA curve on the silica/KX systems, thermal change was confirmed near 400°C to 500°C. Both the DTA and TG curves are changed dramatically between 680°C and 780°C. These changes probably correspond to the melting point of inorganic salts and suggest that the inorganic salt crystals have a partial structural defect in the mixture. In the silica/KI system (Fig. 4c), however, a porous structure could not be formed. To determine why a porous structure did not form would most likely require an examination of the kinetics of the transformation during fusion or sublimation, which is beyond the scope of our present study.

3.4. XRD analysis under high temperature conditions

To elucidate the transformation of the crystalline structure, XRD diffractometry was performed for the silica/KBr system. In Fig. 5, XRD diffraction patterns for the silica/KBr system at various temperatures are illustrated (Fig. 5a). For reference, XRD diffraction pattern

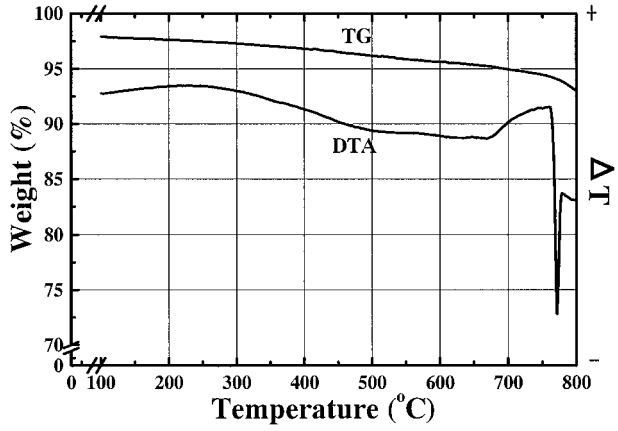

(a)

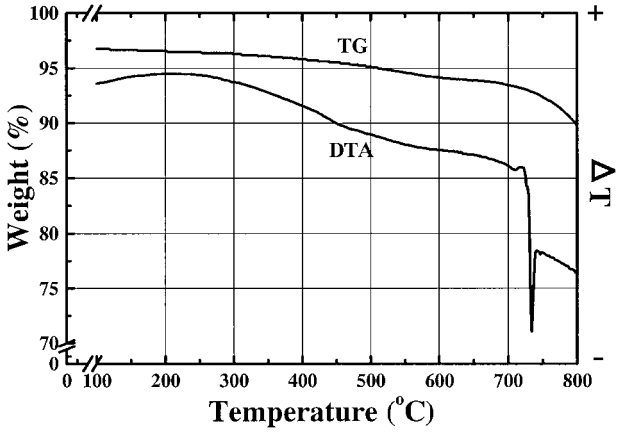

(b)

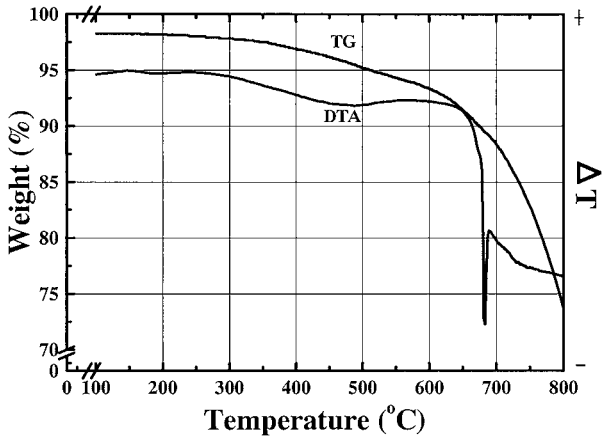

(c)

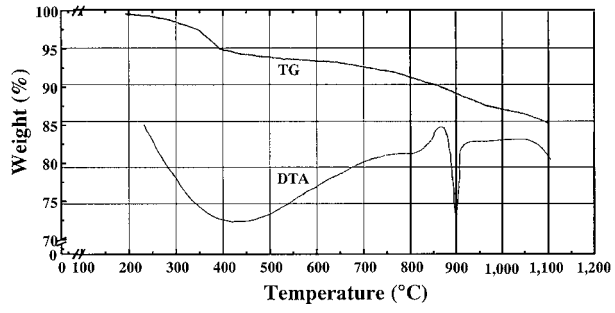

(d)

Figure 4 Thermal analyses (DTA/TG) of silica/KX solid mixture: (a) silica/KCl, (b) silica/KBr, (c) silica/KI, and (d) silica (blank).

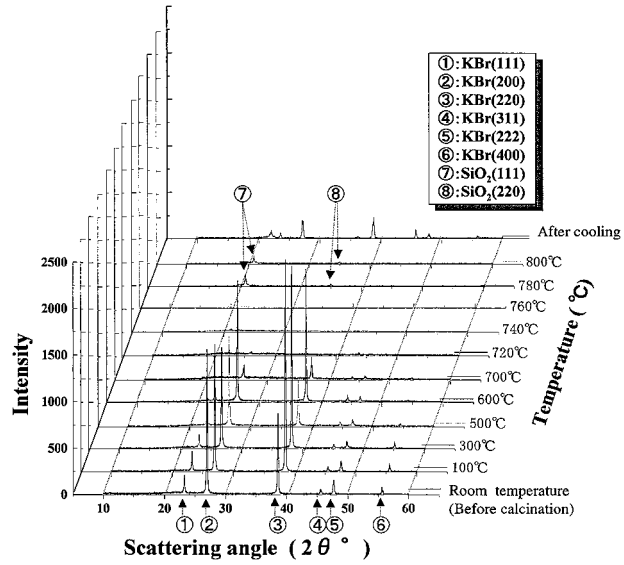

(a)

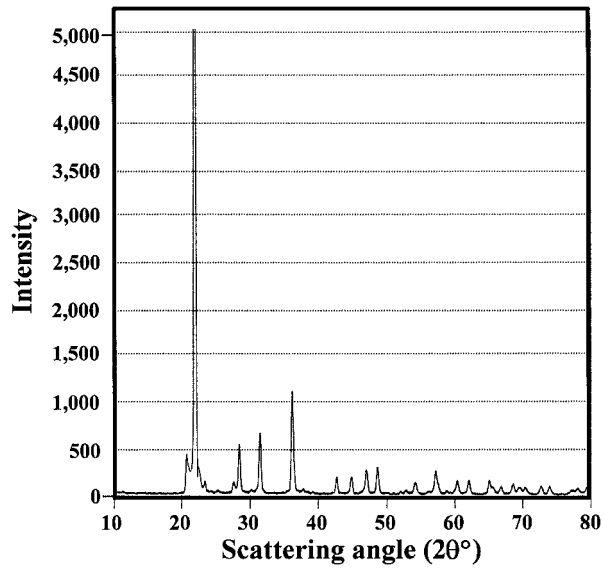

(b)

Figure 5 (a) XRD diffraction patterns of the silica/KBr system at temperatures ranging from room temperature to 800°C. (b) XRD diffraction patterns of the silica after cooling down to room temperature from 800°C.

for the silica after cooling down to room temperature from 800°C is added (Fig. 5b).

Referring to the Joint Committee on Powder Diffraction Standards (JCPDS) files, the diffraction patterns at temperatures ranging from room temperature to near 700°C were ascribed to the KBr crystal. At temperatures higher than 760°C, the newly emerged patterns were attributed to the silica crystal (the cristbalite form) also in reference to the JCPDS files. Furthermore, at temperatures ranging from 720°C to 740°C, no diffraction patterns were detected, indicating neither silica nor KBr had a crystalline structure.

Fig. 6 shows the temperature/interplanar spacing relationship induced from Bragg's reflecting condition (spacing ratio of d/n at each temperature to the one at room temperature: $(d/n)_0$). To avoid overlaps, the curves have been shifted vertically and separated by a factor of 0.05, with the exception of d_{111}. Clearly, all spacing curves had the tendency of increasing with the

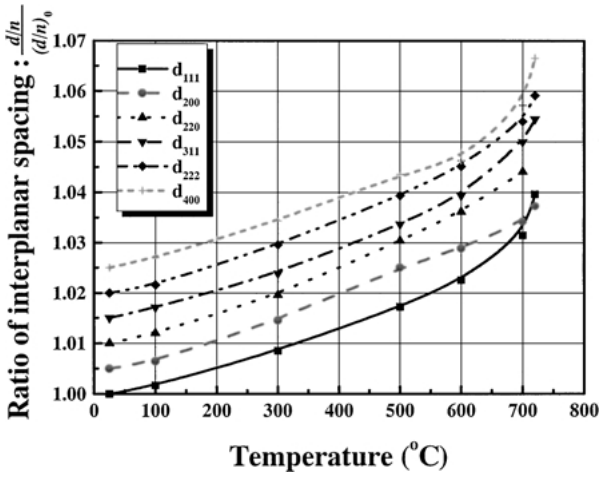

Figure 6 Temperature dependence of interplanar spacing (spacing ration of d/n at each temperature to the one at room temperature: $(d/n)_0$ on KBr crystalline phase in the silica/KBr system. To avoid overlaps, the curves have been shifted verticallly and separated by a factor of 0.05, with the exception of d_{111}.

increase in temperature. More specifically, a remarkable increase was found near 700°C, which suggests that the KBr crystal lattice became loose or partially defected during the calcination process.

3.5. Observation using an environmental scanning electron microscope (ESEM)

ESEM images of the silica/KBr system are shown in Fig. 7. Photographs taken at temperatures ranging from 300°C to 600°C (Fig. 7b–d) indicate that clusters of KBr crystal seemed to have partially disappeared. While in the sample chamber, the fused KBr component was sublimated and eventually was exhausted during observation under a vacuum. Even so, silica lumps were observed to be moving vigorously near 600°C, and then mutually coalesce at temperatures over 700°C (Fig. 7e–g).

3.6. Transformation of state during coagulation/phase separation process

Based on the results above, the transformation of the porous structures is speculated as follows (Fig. 8). As the initial solid mixture of amorphous silica and KX is calcined, the silica particles aggregate in a continuous KX amorphous phase. After aggregating, the silica particles begin coagulate, forming a continuous phase denser than the original particles, without passing through a homogeneous phase. As the temperature decreases, a continuous structure of silica coagulum forms within the KX crystalline phase. After cooling, KX is leached from the calcined species, leaving behind a continuous structure of silica.

Conventionally, porous structures are formed from completely homogeneous states at temperatures ranging from 1400°C to 1700°C, with pore diameter and pore size distribution typically controlled through quenching. However, such cooling tends to produce crystallization, impeding pore control.

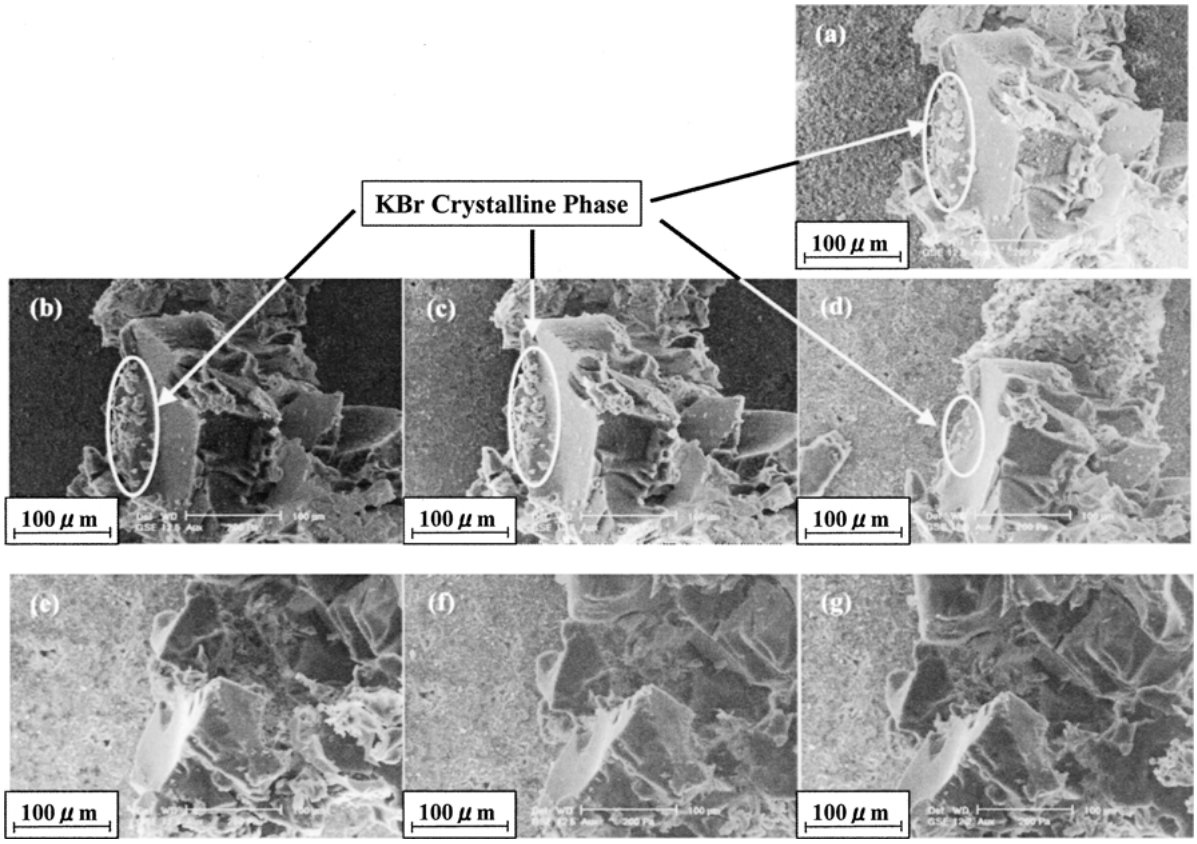

Figure 7 ESEM photographs of the silica/Br system at temperatures ranging from room temperature to 800°C: (a) room temperature, (b) 300°C, (c) 550°C, (d) 600°C, (e)700°C, (f)740°C, and (g) 800°C.

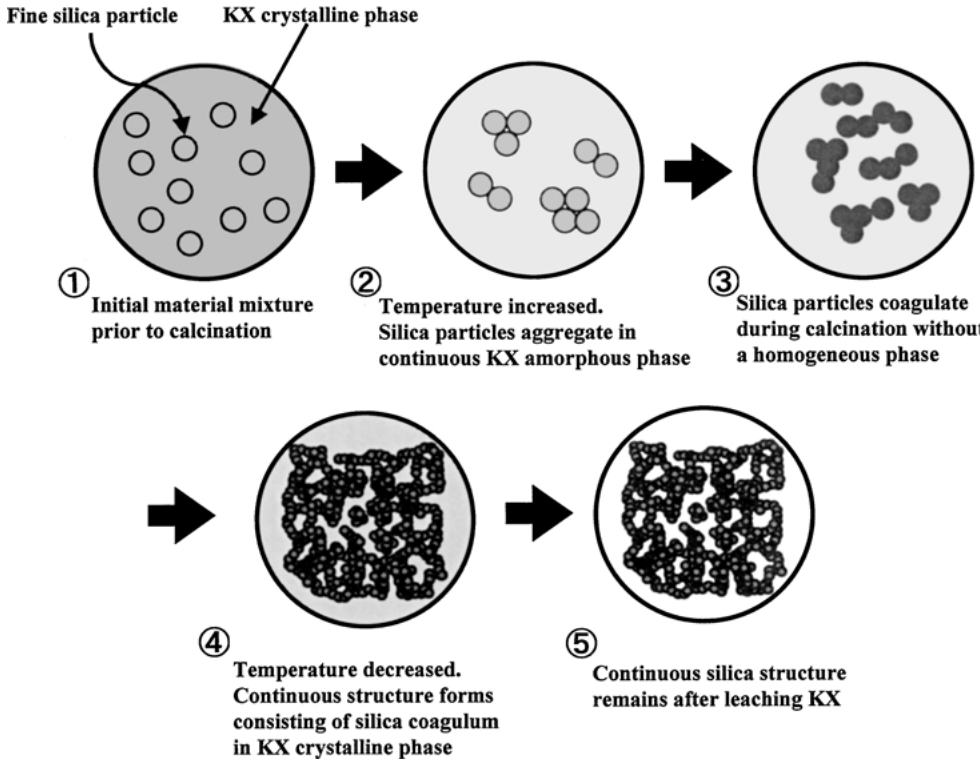

Figure 8 Schematic of coagulation/phase separation process.

4. Conclusions

Porous structures can be constructed by calcining a solid mixture of silica and inorganic salts at temperatures below either of their melting points. During calcination, the crystalline structure of the inorganic salt cluster was observed to partially deform. Then, in the temperature range where inorganic salt and silica existed in amorphous states, "coagulation/phase separation" occurred in that the silica coagulated, effectively separating the phases. The phase separation resulted in a porous silica structure.

This coagulation/phase separation process does not involve a homogeneous state for the two components, but instead separates the system components through structural fluctuations, in effect including coagulation of the silica component while the system remains in a heterogeneous state. Such structural fluctuations were observed with XRD under high temperature conditions, which showed interplanar spacing increased during calcinations of the silica/KX solid mixture, indicating particle deformation of the KX cluster. Such a partial deformation would be expected to possess a lower cohesive energy than the ordered crystalline domain. Furthermore, ESEM showed greater silica mobility with increases in temperature. This increased mobility indicates a decrease in the cohesive energy of the amorphous silica. The lack of a homogeneous state coupled with decreases in the cohesive energy of the two system components suggests silica coagulated, with the individual silica particles binding to each other to form the resultant porous structures.

Ackowledgements

The authors acknowledge the Incorporate Foundation Institute of Research and Innovation for their special consideration regarding the use of the porosity meter. We also specially want to thank Simazu Seisakusho Co. Ltd. for allowing us to use an X-ray diffractometer (XRD-6100), and to Nikon Instech Co. Ltd. for allowing us to use an environmental scanning electron microscope: ESEM. Further thanks to Nissan Chemical Industries, Ltd. for supplying us the colloidal silica sample (Snowtexa^{TM}). Finally, we are grateful to these groups for their interest and stimulating comments on this research.

References

1. W. M. MEIER and D. H. OLSON, "Atlas of Zeolite Structure Types," 3rd ed. (Butterworths-Heinemann, London, 1992).
2. M. E. NORDBERG, *J. Amer. Ceram. Soc.* **l27**, (1944) 299.
3. W. HALLER, D. H. BLACKBURN, F. E. WAGSTAFF and R. J. CHARLES, *ibid.* **53**(1) (1970) 34.
4. T. YAZAWA, *Hyomen* **29**(12) (1991) 971.
5. T. NAKAJIMA and Y. KUROKI, *J. Chem. Soc. Jpn., Chem. Ind. Chem.* **1**(8) (1981) 1231.
6. S. MORIMOTO, *J. Ceram. Soc. Jpn.* **98**(10) (1990) 1093.
7. K. NAKANISHI, *Hyomen* **33**(4) (1995) 240.
8. T. KIJIMA, K. YADA and M. MACHIDA, *ibid.* **36**(1) (1998) 9.
9. A. KAWAHARA, *et al.*, *J. Ceram. Soc. Jpn.* **100**(2) (1992) 212.
10. R. TAKAHASHI, K. NAKANISHI and N. SOGA, *ibid.* **106**(8) (1998) 772.
11. N. YOSHIZAWA, H. HAJIMA and N. YAMADA, *Hyomen* **35**(12) (1997) 652.
12. T. YANAGISAWA, T. SHIMIZU, K. KURODA and C. KATO, *Bull. Chem. Soc. Jpn.* **63** (1990) 988.
13. S. INAGAKI, Y. FUKUSHIMA and K. KURODA, *J. Chem. Soc., Chem. Commun.* (1993) 680.
14. S. INAGAKI, A. KOIWAI, N. SUZUKI, Y. FUKUSHIMA and K. KURODA, *Bull. Chem. Soc. Jpn.* **69** (1996) 1.

15. C. T. KRESGE, M. E. LEONOWICZ, W. J. ROTH, J. C. VARTULI and J. S. BECK, *Nature* **359** (1992) 710.
16. J. S. BECK, J. C. VARTULI, W. J. ROTH, M. E. LEONOWICZ, C. T. KRESGE, K. D. SCHMITT, C. T.-W. CHU, D. H. OLSON, E. W. SHEPPARD, S. B. MCCULLEN, J. B. HIGGINS and J. L. SCHLENKER, *J. Amer. Chem. Soc.* **114** (1992) 10834.
17. T. YAMAGUCHI, T. HOSHI, K. MURATA, S. KANEKO and K. TAKEDA, *J. Min. Mater. Proc. Inst. Jpn.* **115**(2) (1999) 111.
18. T. ARAI, K. IMAIZUMI and K. TAKEDA, in Proceedings of the 2nd International Conference on Processing Materials for Properties, San Francisco, November 2000, edited by B. Mishra (Colorado School of Mines) and C. Yamauchi (Nagoya University) p. 989.
19. T. YAMAGUCHI, T. NAKAI, N. ASANUMA, S. ONO and K. TAKEDA, *J. Min. Mater. Proc. Inst. Jpn.* **115**(6) (1999) 475.
20. T. YAMAGUCHI, T. NAKAI and K. TAKEDA, *ibid.* **115**(11) (1999) 847.
21. T. YAMAGUCHI, T. NAKAI and K. TAKEDA, *ibid.* **116**(1) (2000) 56.
22. K. IMAIZUMI, T. NAKAI, H. SHIRASAKA and K. TAKEDA, in Proceedings of the 2nd International Conference on Processing Materials for Properties, San Francisco, November 2000, edited by B. Mishra (Colorado School of Mines) and C. Yamauchi (Nagoya University) p. 469.

Received 9 January 2002
and accepted 21 January 2003